ELSEVIER
Journal of Molecular Structure 604 (2002) 165–176
Journal of
MOLECULAR
STRUCTURE
www.elsevier.com/locate/molstruc

Structure of *N*,*N*-dimethylhydrazone alkylation products

L.I. Larina*, R.V. Karnaukhova, A.S. Nakhmanovich, V.A. Shagun,
P.E. Ushakov, V.A. Lopyrev

Irkutsk Institute of Chemistry, Siberian Branch, Russian Academy of Sciences, 1 Favorsky St.,
664033 Irkutsk, Russian Federation

Received 19 March 2001; revised 9 May 2001; accepted 9 May 2001

Abstract

Alkylation of 1,1-dimethylhydrazone-4- and -3-pyridinaldehydes has been shown, by means of multinucleus 1D- and 2D NMR spectroscopy and quantum chemistry (ab initio), to proceed exclusively by the pyridine nitrogen atom to form the corresponding pyridinium halides. At the same time, 1,1-dimethylhydrazone benzaldehyde is alkylated to the amine nitrogen with the formation of hydrazonium salts. © 2002 Elsevier Science B.V. All rights reserved.

Keywords: NMR spectroscopy; Ab initio (RHF/6-31G**); Alkylation; Hydrazonium salts

1. Introduction

Dimethylhydrazone derivatives are widely used as syntones in fine organic synthesis [1–3]. The methods of synthesis of biologically active compounds [4–6] and complicated condensed heterocycles [7] have been developed on their base. The chemistry of 1,1-dimethylhydrazones is rather well studied [1]; nonetheless the reactions of their quaternization by alkyl halides have not been sufficiently investigated by now [1,8,9]. The alkylation of dimethylhydrazones leads, usually, to the formation of quaternary salts, containing aldohydrazonium fragment (Me_3N^+–N=CH–). This process has almost no dependence on the substituent's character (its configurational and conformational states) and, as a rule, is not accompanied by dehydrohalogenization or deprotonation [1]. The reactions of 1,1-dimethylhydrazones with propargylbromide and 1,3-dibromopropine, leading to the formation of hydrazonium salts, have been studied earlier [9].

2. Results and discussion

2.1. NMR data

To continue our study of the 1,1-dimethylhydrazones alkylation reactions [9] we have studied the reactions of 1,1-dimethylhydrazone benzaldehyde (**1**) and *N*,*N*-dimethylhydrazone-4- (**4**) and -3-pyridines (**9**) with methylhalides and β-chloropropionic acid. The reactions were held in *iso*-propanol heated to 50°C and led to the formation of the corresponding halides (**2**–**3**, **5**–**8**, and **10**–**11**).

---

* Corresponding author. Present address: UMR 7510, Institute Le Bel, Universite Louis Pasteur, 4 rue Blaise Pascal, 67000 Strasbourg, France. Tel.: +7-3952-46-08-71; fax: +7-3952-39-60-46.

E-mail addresses: larina@chimie.u-strasbg.fr (L.I. Larina), larina@irioch.irk.ru (L.I. Larina).

PII: S0022-2860(01)00646-9

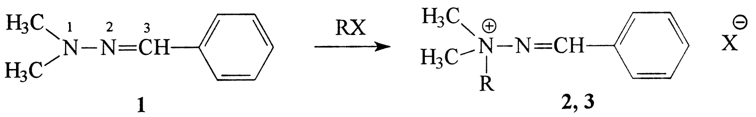

1 **2, 3**

2 R = CH_3; X = I
3 R = CH_2CH_2COOH; X = Cl

The reaction of **1** with methyliodide and β-chloropropionic acid results in the formation of 1,1,1-trimethylhydrazonium iodide (**2**) and 1,1-dimethyl-1-carboxyethylhydrazone benzaldehyde (**3**) with rather high yields. The lowfield displacement of ^{1}H- and ^{13}C chemical shifts of the methyl groups in the product of the reaction in comparison with the initial compound (**1**) (by about 0.8 and 10–13 ppm correspondingly) and the integral intensity analysis proves the formation of the aldohydrazonium fragment containing structure (quaternary nitrogen in the molecule) like **2** or **3** (Table 1). An analogous signal displacement takes place in ^{1}H NMR spectra of quaternary hydrazonium salts [9,10,11]. ^{1}H- and ^{13}C NMR signals of the =CH– fragment undergo much more significant change after quaternization of the nitrogen atom ($\Delta\delta = 1.8$ and 27.5 ppm, correspondingly). The ^{15}N chemical shift values do not change much at the transition to the quaternary salts, taking the ^{15}N NMR scale into consideration (see Table 1). The nature of the alkylating agent (cf. **2** and **3**) has almost no influence on the chemical shifts of the benzaldehyde hydrazonium frame nuclei.

There are at least three nitrogen atoms able to quaternize in the hydrazone molecule (**4**, **9**): N^1 (–NMe_2), N^2 (=N–) and N_{pyr}. One could consider the quaternization of **4** and **9** to proceed by the N^1 atom, i.e. in an analogous way to the reactions of 1,1-dimethylhydrazone benzaldehyde with alkylhalogenides giving the corresponding salts (Table 1).

But the direction of the reaction changes in the hydrazones alkylation. The alkylating agent attacks the pyridine nitrogen atom, to give the corresponding pyridinium salts (**5**–**8** and **10**, **11**). The chemical shift of the pyridine nitrogen atom in the salts, in comparison with the initial molecule (see Table 1), moves to the highfield by more than 100 ppm. The appearance of a singlet of the methyl group at 4.1–4.3 ppm (3H) and a singlet at 3.30 ppm, containing six protons, against nine as in case of **2** (Table 1), also proves the involvement of the pyridine nitrogen into the alkylation reaction. The data of 2D (NOESY) NMR spectroscopy of **8** and **11** also show that the alkylation touches the pyridine nitrogen atom. The protons in positions 2 and 6 have a common cross-peak with the protons of the –N^+–CH_2– fragment. Analogous to **2** and **3**, the nature of the alkylation agent has almost no influence on the NMR spectra parameters of the hydrazone fragment. As it can be seen from Table 1, the nature of the counter-ion has no influence on the salts chemical shifts either.

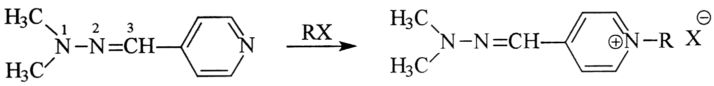

4 **5 - 8**

5 R = CH_3; X = Cl
6 R = CH_3; X = Br
7 R = CH_3; X = I
8 R = CH_2CH_2COOH; X = Cl

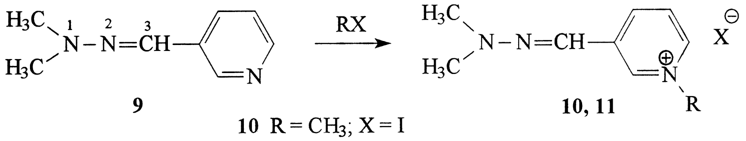

9 **10, 11**

10 R = CH_3; X = I
11 R = CH_2CH_2COOH; X = Cl

Table 1
^{1}H-, ^{13}C- and ^{15}N NMR chemical shifts (in CD_3OD, ^{2}H–H coupling constant (J) = ^3J) (ppm) and J (H–H)^2 (Hz) of alkylation products of *N*,*N*-dimethylhydrazone

No	Compound	δ^1H			δ^{13}C			δ^{15}N		
		$N(CH_3)_2$	N=CH	Others	$N(CH_3)_2$	N=CH	Others	$N(CH_3)_2$	N=CH	N_{Pyr}
1	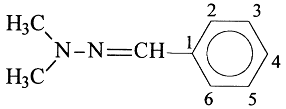	2.82	7.21	7.14 t ($J = 7.5$ Hz) 7.24 t ($J = 7.3$ Hz) 7.51 d ($J = 7.5$ Hz)	43.02	138.00	126.63 C-3,5 128.31 C-2,6 129.31 C-1 134.55 C-4	−274.3	−27.5	–
2	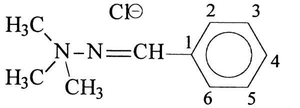	3.57	9.07	7.37 t ($J = 7.8$ Hz) 7.47 t ($J = 7.4$ Hz) 7.68 d ($J = 7.8$ Hz)	56.49	165.51	130.65 C-3,5 131.14 C-2,6 131.84 C-1 135.37 C-4	−281.8	−39.5	–
3	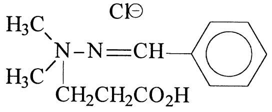	3.58	9.09	2.93 t ($J = 6.8$ Hz) CH_2–CO– 4.10 t ($J = 6.8$ Hz) N–CH_2 7.91–7.55 m Aryl	53.83	166.62	29.22 CH_2–CH_2 66.62 N–CH_2 130.64 C-3,5 131.29 C-2,6 131.93 C-1 135.41 C-4 173.12 C=O	−279.1	−46.6	–
4	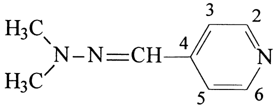	3.04	7.06	7.45 d ($J = 4.7$ Hz) H-3,5 8.33 d ($J = 4.7$ Hz) H-2,6	42.57	126.85	120.68 C-3,5 146.85 C-4 149.82 C-2,6	−266.0	−16.1	−84.5
5	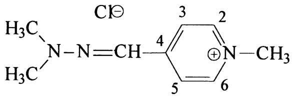	3.30	7.16	4.17 s N_{Pyr}–CH_3 7.84 d ($J = 4.7$ Hz) H-3,5 8.42 d ($J = 4.7$ Hz) H-2,6	43.34	121.99	46.95 N–CH_3 121.42 C-3,5 144.95 C-4 154.46 C-2,6	−243.7	−2.0	−198.4
6	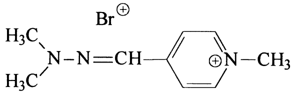	3.31	7.11	4.43 N_{Pyr}–CH_3 7.84 d ($J = 4.8$ Hz) H-3, 5 8.85 d ($J = 4.8$ Hz) H-2, 6	42.76	119.76	46.21 N_{Pyr}–CH_3 120.22 C-4 143.04 C-3, 5 151.63 C-2, 6	−241.9	−1.0	−198.0

Table 1 (*continued*)

No	Compound	δ^1H			$\delta^{13}C$			$\delta^{15}N$		
		$N(CH_3)_2$	N=CH	Others	$N(CH_3)_2$	N=CH	Others	$N(CH_3)_2$	N=CH	N_{Pyr}
7	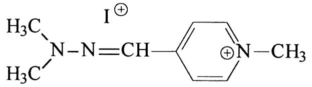	3.32	7.14	4.41 N_{Pyr}–Me 7.85 d ($J = 4.7$ Hz) H-3, 5 8.71 d ($J = 4.7$ Hz) H-2, 6	43.61	120.54	120.80 C-4 143.50 C-3, 5 152.67 C-2, 6	−241.3	−1.1	−197.6
8	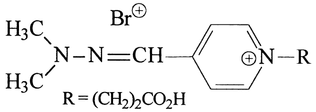	3.30	7.14	3.05 t ($J = 6.8$ Hz) CH_2–CO– 4.61 t ($J = 6.8$ Hz) N_{Pyr}–CH_2 7.82 d ($J = 4.9$ Hz) H-3, 5 8.52 d ($J = 4.9$ Hz) H-2, 6	43.71	122.26	35.80 CH_2–CH_2 56.73 N–CH_2 121.57 C-3, 5 144.88 C-2, 6 155.25 C-4 173.57 C=O	−241.5	−0.7	−189.4
9	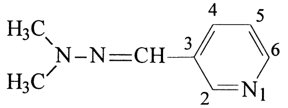	2.930	7.117	7.25 dd H-5 7.88 d H-4 8.29 d H-6 8.63 s H-2	42.72	124.87	128.08 C-5 133.37 C-4 134.84 C-3 147.46 C-2(6) 147.70 C-6(2)	−275.0	−26.8	−68.3
10	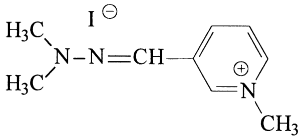	3.15	7.22	4.39 s N_{Pyr}–CH_3 7.90 dd H-5 8.52 d H-4 8.57 d H-6 8.95 s H-2	42.86	121.63	56.50 N_{Pyr}–CH_3 128.67 C-5 139.64 C-4 140.26 C-3 142.23 C-2 154.62 C-6	−260.5	−15.9	−179.8
11	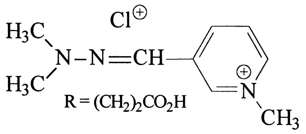	3.15	7.19	3.13 t ($J = 6.8$ Hz) CH_2–CO– 4.85 t ($J = 6.8$ Hz) N_{Pyr}–CH_2 7.90 dd ($J = 8.2$,6.1 Hz) H-5 8.54 d ($J = 8.2$ Hz) H-4 8.69 d ($J = 6.1$ Hz) H-6 9.04 s H-2	42.99	121.81	58.79 N–CH_2 35.77 CH_2–CH_2 129.08 C-5 140.47 C-4 140.73 C-3 142.23 C-2, 6 173.23 C=O	−259.9	−14.8	−169.2

The NMR data can be described taking in consideration the resonance structures of halogenides **5**–**8**:

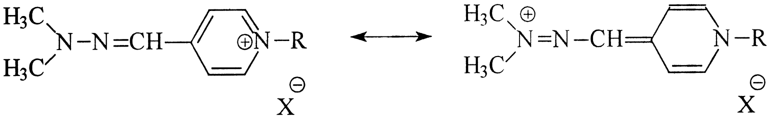

The $\delta\,^1$H value of the NMe fragment (~3.30 ppm) has an intermediate value in comparison to the neutral molecule (**4**) (~3.0 ppm) and the salts (**2**,**3**) (~3.6 ppm), i.e. there is a partial positive (delocalized) charge on the N^1. Besides, the proton shifts of NMe group in the spectra of 3-pyridinium derivatives **10** and **11** have less lowfield displacement ($\delta\,^1$H ~3.15 ppm) in comparison with those of the derivatives of 4-pyridinium **5**–**8**, that may give evidence concerning a smaller delocalization of the positive charge in the molecule of 3-pyridinium, where no analogous resonance structure can be realized. Thus, the charge appearing on the pyridine nitrogen atom as a result of the alkylation **5**–**8**, is delocalized over the whole molecule, causing the change of the chemical shifts of nuclei in all the fragments of the molecule.

To conclude, a global shielding of ^{15}N (highfield shift ~100 ppm) in going from the neutral molecule to its salt, can be a test for quaternization of the pyridine nitrogen atom.

Quantum-chemical analysis of thermodynamical and kinetic characteristics of the electrophilic addition reactions was carried out in order to find out the reasons of absolute inversion of the methylation center on the transition from compound **1** to **4**.

2.2. Ab initio calculations

*2.2.1. Stationary states of compounds **1** and **4** and their relative stability*

Ab initio calculations of hydrazone alkylation taking the medium-effects into consideration were carried out for the more complete picture of quaternization.

The absolute inversion of the active center in the electrophilic addition reactions on turning from the structures **1** to **4** and **9**, according to the orbital-charge and stereochemical characteristics of the centers, is unexpected. An attempt to find out the main reasons for such a change of the reaction channel has been made in this work. We considered the quantum-chemical model of an ionic mechanism of the reaction, whose bimolecular chain can be shown like this.

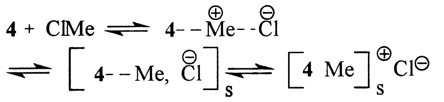

$$4 + \mathrm{ClMe} \rightleftharpoons 4\text{--}\overset{\oplus}{\mathrm{Me}}\text{--}\overset{\ominus}{\mathrm{Cl}} \rightleftharpoons \left[4\text{--}\mathrm{Me},\ \overset{\ominus}{\mathrm{Cl}}\right]_{\mathrm{s}} \rightleftharpoons \left[4\ \mathrm{Me}\right]_{\mathrm{s}}^{\oplus}\mathrm{Cl}^{\ominus}$$

The study of the main processes of alkylhalogenation was made with ab initio (RHF/6-31G**) calculations. Methyl chloride was used as the alkylation agent.

Three stationary states (not taking the pseudodegenerate ones into consideration) corresponding to the minimum of complete energy ($\lambda = 0$) and separated by activation parameters exceeding 6 kcal/mol have been found on the potential surface of conformational changes for both **1**- and **4**-like structures.

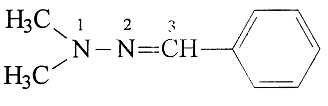

1

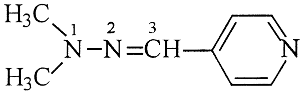

4

Structures **1a** and **4a** are the most stable with the *trans*-configuration of the N–N–C–C chains and the planar structure of the frame (Fig. 1). These structures are more polar states among the considered rotamers (Table 2). The least stable forms (**1b** and **4b**) with *cis*-configuration of the central chains also have a planar structure of the heavy atoms frame. Significant deformation of the valence angle of the central frame (Fig. 1) is a destabilizing factor in these structures, that, in its turn, allows to save the stabilizing character of the conjugation effect among the π-systems of the central frame and of the cyclic substituent.

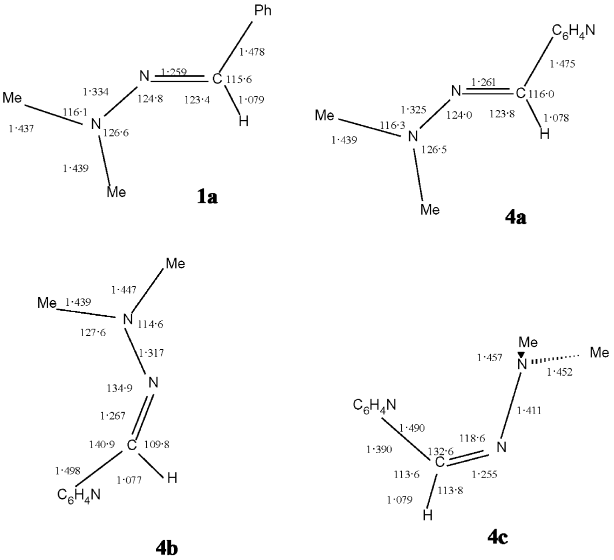

Fig. 1. Molecular structures and geometrical characteristics of the main stationary states of **1** and **4** calculated by ab initio (RHF/6-31G**). Here, and in Figs. 2–4 the bond lengths are in Å, and the angles in degrees.

Obviously, the N^2-center, in the case of 'chemically noticeable' accumulation of rotamers **1b** and **4b** in the reaction mixture, can be an alternative for the electrophilic attack, along with N^1- and N_{pyr} centers, because of the improvement of stereochemical conditions caused by the weakening of its shielding by the substituent. The third, the least polar local stationary condition **c** remains in a *cis*-configuration of the central chain and is intermediate in stability among the two first rotational forms (Fig. 1, Table 2). The substituent R (being planar in the range of 0.1 Å) has angles of rotation, relative to the plane of the central frame, of 25.1 and 23.4°, for **1c** and **4c**, respectively. Structures **c** do not have the stabilizing effect of conjugation (the equalization of bonds is much less noticeable, than in the analogs **a** and **b** (Fig. 1)), while the deformation of valent angles of the central frame in the structure **c** is not as much as in **b**. The pyramidal degree of the N^1-atom grows significantly. The movement of the N^1-atom out of the plane of valently bonded to it atoms for the rotamers **a** and **b** does not exceed 0.1 Å, and is 0.497 and 0.458 Å for **1** and **4**, respectively. As a result of such structural deformation the steric shielding of N^1-atom by the methyl substituents noticeably falls, and its potential ability to interact with the methyl cation has to grow. However, the real existence of **1** and **4** in the form **b** or **c** is hardly possible taking into consideration the energetic characteristics of rotamers (Table 2) and activation parameters of their mutual transitions ($E_{a\rightarrow b} = -53.4$ kcal/mol (**1**) and 51.9 kcal/mol (**4**)). Active participation of external agents, or a transition into solid state, or their initial formation in the reaction mixture by choosing the used reagents and varying the reaction conditions is necessary to achieve this. Taking the obtained conformational results into consideration, the structure **a** was the initial (or starting) structure in all the following calculations (unless it is specially noted).

Table 2
The complete energy (E_{compl}, a.u.) (1 a.u. = 627.5095 kcal/mol), relative energy (ΔE, kcal/mol), dipole moment (μ, D) of isolated states of stable rotamers of **1**, **4** and CH_3Cl, predicted by ab initio method (SCF/6.31G**)

Structure	State	E_{compl}	ΔE	μ
1	**a**	−456.636988	0.0[a]	1.91
	b	−456.611464	16.0[a]	1.53
	c	−456.632759	2.6[a]	1.69
4	**a**	−472.631550	0.0[b]	4.86
	b	−472.605276	17.5[b]	3.17
	c	−472.628452	1.9[b]	1.38
CH_3Cl		−499.097899		2.25

[a] Relative to the structure **1a**.
[b] Relative to the structure **4a**.

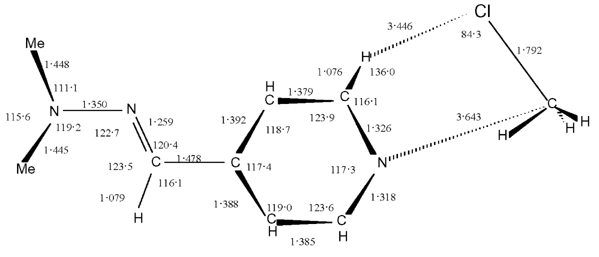

12a

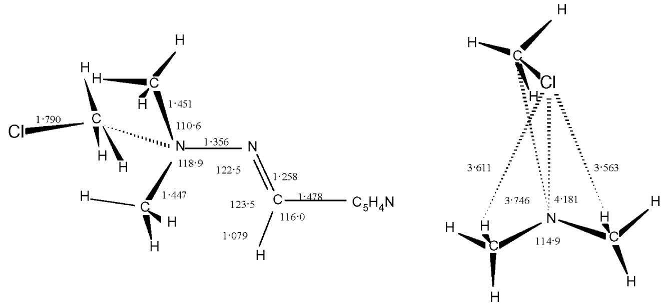

12b

Fig. 2. Molecular structures and geometrical characteristics of associates **12a** and **12b** (in two projections: front and side views).

2.2.2. Structure and relative stability of the associates

Among potentially possible centers of attack of **4** by the methyl cation it is possible to find the π-system of the pyridine substituent, the π-bond N=C and lone pairs of N^1-, N^2-, and N_{pyr}-atoms. However, there are no experimental proofs of the possible methylation of the first three 'objects'. The search of possible stationary states of associates **12** was made based on the assumption of the possible attack of N^1- or N_{pyr}-centers by the alkyl-cation. As the calculations have shown, there are, on the potential surface of intermolecular interaction, at least two stationary states, corresponding to the linked structures ($\lambda = 0$), whose geometrical characteristics are given in Fig. 2. The differences between relative stability of structures **12a** and **12b** are insignificant. Structure **12a**, where methylchloride is coordinated with the pyridinium part of dimethylhydrazone, turned out to be more advantageous. It is by 0.7 kcal/mol more stable than **12b**. This fact, somehow, indicates the 'initial' equality of N^1- and N_{pyr}-centers alkylation. Both complexes are thermodynamically more stable than the isolated fragments **4a** and CH_3Cl by 19.2 and 19.7 kcal/mol for **12b** and **12a**, respectively. The degree of mutual influence of dimethylhydrazone and methylchloride in the associates, from the point of view of charge transfer, is insignificant. The charge transfer in both cases is small (-0.007 and $-0.014e$ at ClMe, respectively for **12b** and **12a**).

2.2.3. Pyridinium and aldohydrazonium cations

Analysis of structural characteristics and relative stability of isolated pyridinium $[NMe_2–NCH–C_5H_4NMe]^+$ (**13a**) and aldohydrazonium $[NMe_3–NCHC_6H_4N]^+$ (**13b**) cations shows the absolute energetic preference of the pyridinium cation, which is by more 23.4 kcal/mol stable than its aldohydrazonium analog (Table 3). Both cations in their optimal stationary state ($\lambda = 0$) (Fig. 3) have planar structure in their heavy atoms frame. The most significant structural response of deformational distortion of **13a** and **13b** is seen in the N–N–C–C chain. For **13b** this is shown by a significant increase of N–N bond length (from 1.325 to 1.448 Å) and decrease of valent angle NNC (from 124.0 to 117.7°). The other

Table 3

Full energy (E_{full}, a.u.), relative energy (ΔE, kcal/mol), number of negative self-values of gessian (λ) of structures **12**–**17**, predicted by the SCF/6.31G** method

Structure	E_{full}	ΔE	λ	Structure	E_{full}	ΔE	λ
12a	−971.75921	0.0[a]	0	**14b**	−971.73848	13.0[a]	0
12b	−971.75816	0.7[a]	0	**15a**	−971.72536	29.4[a]	0
13a	−512.06816	0.0[b]	0	**16b**	−971.68224	48.3[a]	1
13b	−512.03093	23.4[b]	0	**16a**	−971.68989	43.5[a]	1
6a	−971.70152	36.2[a]	0	**9a**	−971.66423	59.6[a]	1

[a] Relatively to structure **12a**.

[b] Relatively to structure **13a**.

structural parameters, on the whole, do not undergo significant changes (Figs. 1 and 3).

Structural characteristics of **13a** cation should have revealed the quaternary nitrogen atom character in the pyridinium fragment. However, the calculations show that the 'head' nitrogen atom obtains more quaternary character as a result of addition of alkyl cation to the pyridinium nitrogen atom. The length of the N–N bond shortens (from 1.325 to 1.282 Å) and of the N^2–C^3 lengthens (from 1.261 to 1.287 Å) (Fig. 3). A significant shortening of the C–R bond length (from 1.475 to 1.441 Å) also takes place. On the whole, the structure of cation **13a** shows that the quaternization, as a result of geometrical reorganization, takes place in the 'head' part of the molecule, despite the addition of the methyl cation to the pyridinium fragment.

Comparative analysis of effective charge shows that its localization on the atoms N^1 and N^2 is much less than on the N_{pyr} one (by 0.43 and 0.29*e*, respectively, (**13a**), cf. 0.03 and 0.16*e* (**13b**)), that, along with the structural data, also proves possibly preferable formation of quaternary salts of **c**-type, not **b**-ones.

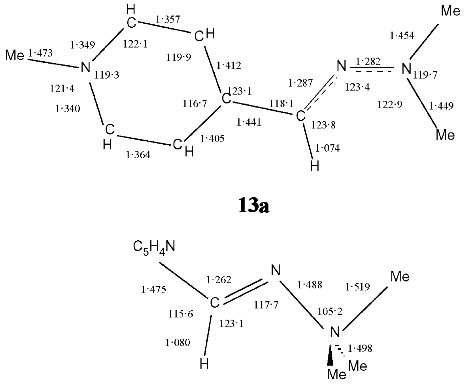

13a

13b

Fig. 3. Molecular structures and geometrical parameters of pyridinium (**13a**) and aldohydrazonium (**13b**) cations.

2.2.4. Structure and lability of $[Me_2N{-}NCHC_5H_4NMe]^{+\cdot}Cl^-$ *and* $[Me_3N{-}CHC_5H_4N]^{+\cdot}Cl^-$ *ionic pairs*

As the calculations have shown, there are several stationary states, corresponding to the linked structures of a pyridinium cation and a chloride anion on the surface of potential energy. The main stationary

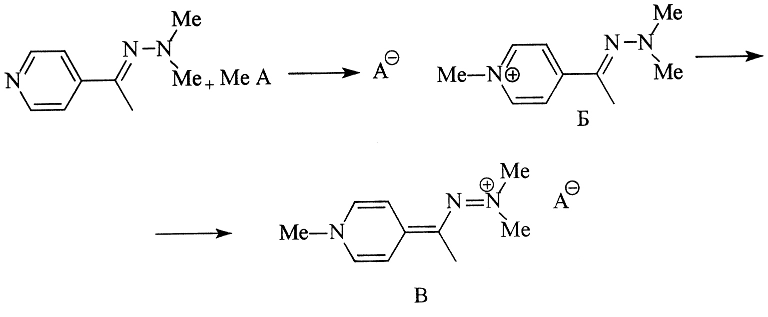

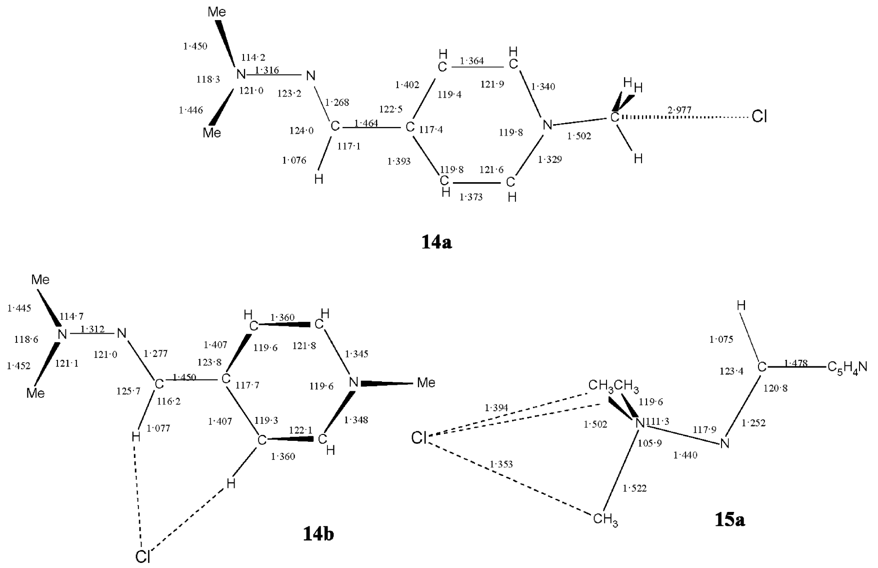

Fig. 4. Main geometrical characteristics of ionic pairs [Me$_2$N–NCHC$_5$H$_4$NMe]$^{+\cdot}$Cl$^-$ (**14a**, **14b**) and [Me$_3$N–CHC$_5$H$_4$N]$^{+\cdot}$Cl$^-$ (**15a**).

state, obtained as a result of alkyl attack along the gradient path connecting the associate (**12a**, Fig. 2) and the ionic pair (**14a**, Fig. 4) through the saddle structure (**14a**, Fig. 5) ($\lambda = 1$), is not the most stable. The more stable are the stationary states **14b** ($\lambda = 0$) (Fig. 4)

Structure **14a** can become structure **14b** along the continuous gradient path through the limiting, for this path, transition state (**16b**, Fig. 5), ($\lambda = 1$). At the same time, in spite of rather significant structural deformations of the cation in the chloride-ion migration (from structures of **b**-type to those of **a**-type), energetically, this process is very 'soft' and is not conjugated with overcoming high energetic barriers (Table 3, Fig. 5).

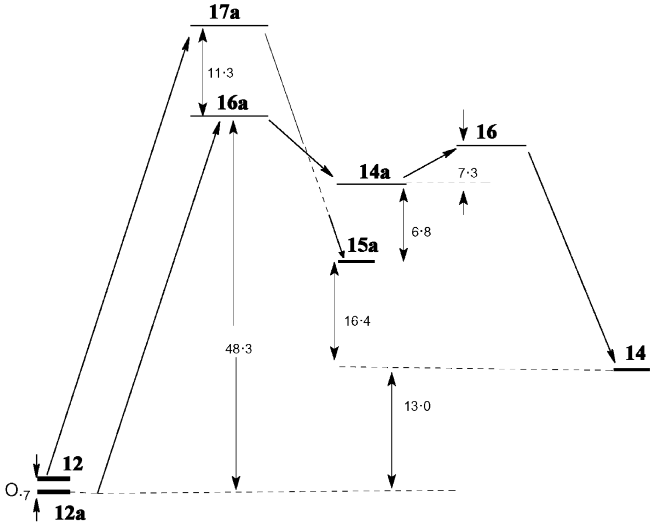

Fig. 5. Schematic picture of energetic evolution on the interaction of alkylchloride with **4** on N^1-(**12b** → TS(**17a**) → **15a**) and N$_{pyr}$-(**12a** → TS(**16a**) → → **14a** → TS(**16b**) → **14b**) centers. The values of relative energy are in kcal/mol.

For the aldohydrazonium and chloride ionic pair, unlike the pyridinium and chloride one, the main stationary state obtained as a result of alkyl attack along the gradient path connecting the associate (**12b**, Fig. 2) and the ionic pair (**15a**, Fig. 4) through the saddle structure (**17a**, Fig. 5), is, according to the results of calculations, the most stable. The stability of pair **15a** though is more stable than the stationary state **14a** by 6.8 kcal/mol, but noticeably worse than ionic pair **14b** ($E_{\mathbf{Xva-XIVa}} = 16.4$ kcal/mol). This leads to the fact that alkylation on N_{pyr} becomes more advantageous, due to low-energy pseudoanisotropic rearrangement. The relation of kinetic parameters ($\Delta E_{\mathbf{17a-16a}} = 11.3$ kcal/mol) also proves this fact.

In the end, we find it necessary to note the potential possibilities of the initial express-analysis of the surface of potential energy by semi-empirical methods. Quantitatively, AM1-calculations are closer to the obtained ab initio calculations. However, both AM1 and PM3-models show the presence of only two stationary states (**a** and **c** analog) in the neutral structures **1** and **4**. The presence of the planar stable form (**b**-analog) is not predicted by semi-empirical methods. The sequence of relative stability of the studied structures is given correctly by AM1-model only, and both models reflect the quantitative character of structural changes, caused by quaternization of the nitrogen atom in the pyridinium cation. So, it is reasonable to use AM1-method for express-analysis of possible reaction-paths of electrophilic addition or substitution in **4** and **9**-like compounds.

As it is seen from the calculations, the experimentally stated selective participation of different centers of compounds **1** and **4** in the reaction of alkylation, shown by the quantum-chemical calculations, can be explained by higher stability of correspondent pyridinium salts. The stability of the latter is caused by partial delocalization of charge involving the N^1 nitrogen atom.

3. Experimental

3.1. NMR and non-empirical calculations

^1H-, ^{13}C-, and ^{15}N NMR spectra were obtained with a Bruker DPX-400 spectrometer with working frequency 400, 100.6 and 40.56 MHz, respectively. HMDS was used as an internal standard for ^1H- and ^{13}C measurements and CH_3NO_2 for ^{15}N. The error in the measurement of chemical shifts of ^1H-, ^{13}C-, and ^{15}N is 0.01, 0.01, and 0.05 ppm, respectively. The constants of spin–spin interaction were measures with precision of 0.1 Hz. The correspondence of signals in **8** and **9** was made with the help of 2D $^1H-^1H$ spectra. The DEPT method was used to assign the signals in ^{13}C NMR spectra. The assignment $\delta\,^{15}N$ was made on the base [12]. IR spectra were recorded with a Specord IR-75.

The non-empirical calculations were made by the limited Hartree–Fock method (RHF) [13,14] in valent-split basis 6-31G** with the use of Gaussian-98 [15]. The complete optimization of the molecular systems geometry, corresponding to the intermediate structures ($\lambda = 1$, where λ is the number of negative self-values of the Gesse matrix in the given stationary point [16] and energetic minimum ($\lambda = 0$, on the surface of potential energy) was done up to the value of the gradient of 10^{-5} Hartree/Bohr. The calculation of the force constants matrix was done analytically with the built-in GAUSSIAN program. The initial view of the surface of potential energy was done with semi-empirical methods AM1 [17,18] and PM3[19]. The structure identification, corresponding to the energetic minimum on the surface of potential energy was done by moving along the gradient line (by the method of the shortest descent) from the saddle point to the next critical point, that allowed to find the gradient reaction path correctly [16]. Near the stationary states the structures were optimized by means of the Newton–Rafson method in Borni's scheme. The superpositional error [20] was not taken into consideration, since only interassociative ways of the reaction were concerned. Moreover, in the chosen for the calculations basis, as the practice of non-empirical calculations shows, the superpositional error is negligible [21]. The necessity of taking the superpositional error into consideration is disputable, since its consideration in a number of cases leads to significant errors in the evaluation of the energy of complex formation [22,23].

3.2. Synthesis of the compounds

*3.2.1. 1,1-Dimethylhydrazone benzaldehyde (**1**)*

It was obtained using the method described in work

[4]. The boiling point is 98–100°C (3 mmHg). According to the literature, the boiling point is 100°C (3 mmHg).

*3.2.2. 1,1,1-Trimethylhydrazone benzaldehyde iodide (**2**)*

3.8 g (0.027 mol) of methyliodide was added to the solution of 4.0 g (0.027 mol) of 1,1-dimethylhydrazone benzaldehyde in 20 ml of *iso*-propanol on cooling (0°C), then the mixture was heated on a water bath up to 55–60°C and stirred for 0.5 h. After this, it was cooled to 0°C and the solid formed was filtered out and dried in vacuum. The yield is 5.0 g (64%). It is white crystals with a melting point of 223–224°C. IR spectrum (KBr), ν, cm^{-1}: 2910, 2840, 1610, 1570, 1460, 1380, 1220, 1170, 1010, 960, 840, 760, 690. Found, %: C 41.16; H 5.16; N 9.62; I 43.65. $C_{10}H_{15}N_2I$. Calculated, %: C 41.38; H 5.17; N 9.65; I 43.79.

*3.2.3. 1,1-Dimethyl-1-carboxyethylhydrazone benzaldehyde chloride (**3**)*

3.0 g (0.02 mol) of 1,1-dimethylhydrazone benzaldehyde were added to 15 ml of absolute acetonitrile; the solution of 2.3 g (0.2 mol) of β-chloropropionic acid in 15 ml of absolute acetonitrile was slowly added at 20°C on stirring. The reaction mixture was heated up to 50°C and stirred for 7 h. The solvent was evaporated, and the residue was refluxed in vacuum. The yield is 3.9 g (76%). The boiling point is 92–94°C (5 mmHg). IR spectrum (microlayer), ν, cm^{-1}: 2970, 2850, 2780, 1705, 1630, 1595, 1570, 1450, 1380, 1250, 1150, 1040, 935, 760, 700. Found, %: C 55.80; H 6.74; Cl 14.05; N 10.67. $C_{12}H_{17}ClN_2O_2$. Calculated, %: C 56.14; H 6.63; Cl 13.84; N 10.92.

*3.2.4. 1,1-Dimethylhydrazone pyridine-4-aldehyde (**4**)*

It was obtained using the method described in work [4]. The boiling point is 64–65°C. According to the literature [4] the boiling point is 65–66°C.

*3.2.5. 1-Methyl-4-(1,1-dimethylhydrazonomethylen)-pyridinium chloride (**5**)*

Gaseous methylchloride was slowly run through the solution of 5.0 g (0.033 mol) of 1,1-dimethylhydrazone pyridine-4-aldehyde in 15 ml of absolute *iso*-propanol during 4 h, then the mixture was heated up to 50°C on the water bath and stirred for 0.5 h. The solvent was evaporated and the solid formed was washed on a filter with cold *iso*-propanol. The yield is 4.0 g (59.6%). The melting point is 105–107°C. IR spectrum (KBr), ν, cm^{-1}: 3420, 3050, 1650, 1560, 1530, 1390, 1200, 1100, 1050, 890. Found, %: C 53.86; H 7.15; Cl 18.13; N 20.95. $C_9H_{14}ClN_3$. Calculated, %: C 54.13; H 7.02; Cl 17.79; N 21.05.

*3.2.6. 1-Methyl-4-(1,1-dimethylhydrazonomethylen)-pyridinium bromide (**6**)*

Gaseous methylbromide was slowly run through the solution of 5.0 g (0.033 mol) of 1,1-dimethylhydrazone pyridine-4-aldehyde in 15 ml of absolute *iso*-propanol during 2 h on cooling (0°C), then the mixture was heated at 50°C for 2 h on the water bath. The solvent was evaporated, cooled to 0°C and the solid formed was washed on a filter with cold *iso*-propanol. The yield is 7.1 g (87%). It is yellow crystals with a melting point of 108–109°C. IR spectrum (KBr), ν, cm^{-1}: 3460, 3040, 1650, 1530, 1480, 1385, 1195, 1095, 1030, 870. Found, %: C 43.84; H 6.05; Br 32.70; N 17.01. $C_9H_{14}BrN_3$. Calculated, %: C 44.26; H 5.74; Br 32.79; N 17.21.

*3.2.7. 1-Methyl-4-(1,1-dimethylhydrazonomethylen)-pyridinium iodide (**7**)*

3.8 g (0.027 mol) of methyliodide was added by drops to the solution of 4.0 g (0.027 mol) of 1,1-dimethylhydrazone pyridine-4-aldehyde in 10 ml of absolute *iso*-propanol at 0°C, then the mixture was heated up to 50°C on the water bath and stirred for 0.5 h; then at 20°C for 2 h. The solvent was evaporated, and the solid formed was filtered, washed on a filter with cold *iso*-propanol, and dried in vacuum. The yield is 6.0 g (77%). The melting point is 113–115°C. IR spectrum (KBr), ν, cm^{-1}: 3420, 3020, 1610, 1570, 1540, 1380, 1060, 670. Found, %: C 37.46; H 4.99; N 14.60; I 43.98. $C_9H_{14}N_3I$. Calculated, %: C 37.11; H 4.81; N 14.43; I 43.64.

*3.2.8. 1-Carboxyethyl-4-(1,1-dimethylhydrazonomethylen)pyridinium chloride (**8**)*

1.41 g (0.013 mol) of β-chloropropionic acid was slowly added to 2.0 g (0.013 mol) of 1,1-dimethylhydrazone pyridine-3-aldehyde in 10 ml of absolute acetonitrile on stirring, the mixture was heated up to 55°C on a water bath and stirred for 7 h. Then it was cooled to 0°C and the solid formed was filtered and washed on a filter with cold acetonitrile. The yield is 3.32 g (90%), it is yellow crystals with melting point of 188–190°C. IR spectrum (KBr), ν, cm^{-1}: 3420, 3110, 3000, 1705, 1630, 1505, 1180, 1080, 880. Found, %: C 50.96; H 6.40; Cl 14.02; N 16.08. $C_{11}H_{16}ClN_3O_2$. Calculated, %: C 51.26; H 6.21; Cl 13.78; N 16.31.

*3.2.9. 1,1-Dimethylhydrazone pyridine-3-aldehyde (**9**)*

It was obtained by the method described in work [4]. The boiling point is 112–114°C (3 mmHg). According to the literature [4], the boiling point is 138°C (10 mmHg).

*3.2.10. 1-Methyl-3-(1,1-dimethylhydrazonomethylen)pyridinium iodide (**10**)*

It was obtained in a similar way to **8**. The yield is 77%. The melting point is 137–139°C (from acetonitrile). IR spectrum (KBr), ν, cm^{-1}: 3420, 3020, 1610, 1570, 1540, 1380, 1060, 670. Found, %: C 37.46; H 4.99; N 14.60; I 43.98. $C_9H_{14}N_3I$. Calculated, %: C 37.11; H 4.81; N 14.43; I 43.64.

*3.2.11. Pyridinium 1-carboxyethyl-3-(1,1-dimethylhydrazonomethylen) (**11**)*

It was obtained analogously to **9**. The yield is 54%. It is yellow crystals with the melting point of 183–185°C. IR spectrum (KBr), ν, cm^{-1}: 3460, 3200, 3060, 1700, 1605, 1550, 1410, 1400, 900, 810, 800, 690. Found, %: C 50.95; H 6.06; Cl 14.11; N 15.94. $C_{11}H_{16}ClN_3O_2$. Calculated, %: C 51.26; H 6.21; Cl 13.79; N 16.31.

Acknowledgements

The authors are grateful to Dr J.-P. Kintzinger for fruitful discussions of the present results and his hospitality in the NMR Laboratory of Condensed Matter (Universite Louis Pasteur, 4, rue Blaise Pascal, 67000 Strasbourg, France) in the frame of a Post Doctoral Grant (L.I.L.) from Rhodia. We thank Dr J.-R. Desmurs (Rhodia Organique, Pharmaceutical Ingredients, Etoile Part-Dieu, 190, avenue Thiers, 69457 Lyon Cedex 06, France) and Dr G. Dolgushin (Irkutsk Institute of Chemistry SB RAS, Russia) for helpful comments.

References

[1] Yu.P. Kitaev, B.I. Buzykin, Hydrazony, Nauka, Moskwa, 1974.

[2] P.A.S. Smith, E.E. Most, J. Org. Chem. 22 (1957) 358.

[3] D.E. Morrow, N.E. Batler, E. Hoang, J. Org. Chem. 30 (1965) 579.

[4] D.A. Clarke, R.K. Barclay, C.C. Stock, C.S. Rondestvedt, J. Proc. Soc. Expt. Biol. Med. 90 (1955) 484.

[5] R.H. Wiley, S.C. Slaywaker, H. Kraus, J. Org. Chem. 22 (1957) 204.

[6] Pat USA 3362994, Ref. Zh. Khim. 1970 (1968) 1N740.

[7] A.B. Koldobskii, V.V. Lunin, S.A. Voznesenskii, Zh. Org. Khim. 28 (1992) 809.

[8] L.I. Larina, R.V. Karnaukhova, V.A. Shagun, A.S. Nakhmanovich, P.E. Ushakov, V.A. Lopyrev, 17th International Congress of Heterocyclic Chemistry, Vienna, Austria, 1–6 August 1999, Abstract, PO 298.

[9] V.N. Elokhina, A.S. Nakhmanovich, R.V. Karnaukhova, L.I. Larina, V.A. Lopyrev, Zh. Org. Khim. 36 (2000) 502.

[10] A.Yu. Chervinskii, A.N. Vdovichenko, S.P. Kobzev, L.M. Kapkan, Zh. Org. Khim. 32 (1996) 529.

[11] V.A. Lopyrev, K.A. Volkova, L.I. Larina, B.F. Kukharev, Zh. Org. Khim. 36 (2000) 39.

[12] M. Witanowski, G.A. Webb, Nitrogen NMR, Plenum, New York, 1973.

[13] V.I. Minkin, B.Ya. Simkin, R.M. Minyaev, Quantum Chemistry of Organic Compounds. Mechanisms of Reactions, Springer, Berlin, 1990.

[14] W.J. Hehre, L. Radom, P.V.R. Schleyer, J.A. Pople, Ab initio Molecular Orbital Theory, Wiley, New York, 1986.

[15] M.J. Frisch, G.W. Trucks, H.B. Schlegel, G.E. Scuseria, M.A. Robb, J.R. Cheeseman, V.G. Zakrzewski, J.A. Montgomery, Jr., R.E. Stratmann, J.C. Burant, S. Dapprich, J.M. Millam, A.D. Daniels, K.N. Kudin, M.C. Strain, O. Farkas, J. Tomasi, V. Barone, M. Cossi, R. Cammi, B. Mennucci, C. Pomelli, C. Adamo, S. Clifford, J. Ochterski, G.A. Petersson, P.Y. Ayala, Q. Cui, K. Morokuma, D.K. Malick, A.D. Rabuck, K. Raghavachari, J.B. Foresman, J. Cioslowski, J.V. Ortiz, B.B. Stefanov, G. Liu, A. Liashenko, P. Piskorz, I. Komaromi, R. Gomperts, R.L. Martin, D.J. Fox, T. Keith, M.A. Al-Laham, C.Y. Peng, A. Nanayakkara, C. Gonzalez, M. Challacombe, P.M.W. Gill, B. Johnson, W. Chen, M.W. Wong, J.L. Andres, C. Gonzalez, M. Head-Gordon, E.S. Replogle, J.A. Pople, GAUSSIAN 98, Revision A.6, Gaussian, Inc., Pittsburgh PA, 1998.

[16] P.M. Minyaev, Russ. Chem. Rev. 63 (1994) 883.

[17] M.J.S. Dewar, E.G. Zoebisch, E.F. Healy, J.J.P. Stewart, J. Am. Chem. Soc. 107 (1985) 3902.

[18] M.J.S. Dewart, E.G. Zoebisch, J. Mol. Struct. 189 (1988) 1.

[19] J.J.P. Stewart, J. Comput. Chem. 10 (1989) 209.

[20] R. Cammi, R. Bonaccorsi, J. Tomasi, Theor. Chim. Acta 68 (1985) 271.

[21] F.B. van Duijneveldt, J.G.C.M. van Duijneveldt-vante Rijdt, J.H. van Lenthe, Chem. Rev. 94 (1994) 1873.

[22] P. Valiron, A. Vilok, I. Mayer, J. Comput. Chem. 14 (1993) 401.

[23] D.B. Cook, T.L. Sordo, J.A. Sordo, J. Chem. Soc. Chem. Commun. (1990) 485.